Archives of Materials Science and Engineering
Volume 123
Issue 1
September 2023
Pages 5-12
International Scientific Journal
published monthly by the
World Academy of Materials
and Manufacturing Engineering

DOI: 10.5604/01.3001.0053.9750

Influence of manganese content on the microstructure and properties of AlSi10MnMg(Fe) alloy for die castings

J. Piątkowski [a,*], M. Hejne [b], R. Wieszała [c]
[a] Faculty of Material Engineering, Silesian University of Technology,
ul Krasińskiego 8, 40-019 Katowice, Poland
[b] Magna Casting Poland, sp. z o.o., ul. Szkolna 15, 47-225 Kędzierzyn-Koźle, Poland
[c] Faculty of Transport and Aviation Engineering, Silesian University of Technology,
ul Krasińskiego 8, 40-019 Katowice, Poland
* Corresponding e-mail address: jaroslaw.piatkowski@polsl.pl
ORCID identifier: https://orcid.org/0000-0003-3602-4605 (J.P.)

ABSTRACT

Purpose: This paper was to determine the effect of different manganese addition contents from 0.2 to 1.0 wt.% on the microstructure, HB hardness and selected mechanical properties (UTS; YS; EL) of AlSi10MnMg alloy with increased iron content (about 1.0 wt.%). The proportion of iron in the studied alloy is so high because approx. 50% of the charge came from secondary materials.

Design/methodology/approach: Chemical composition tests were performed using a Foundry Master Compact 8 emission spectrometer. Static tensile testing at ambient temperature was carried out according to PN-EN ISO 6892-1 on an Instron 3382 using a 20:1 ratio and a constant tensile speed of 5 mm/min^{-1}. Tensile strength (UTS), conventional yield strength (YS), and per cent elongation after rupture of a proportional sample (EL) were determined from this test. Brinell hardness measurement was performed on a Zwick ZHF1, with a loading force of 250 N, with a 5 mm diameter ball for 35 s. Ten measurements were taken, discarding the two outliers, and the arithmetic mean was calculated from the remaining measurements. Metallographic studies were conducted on a MeF-2 Reichert light microscope. X-ray microanalysis studies were carried out on a Hitachi S-3400 scanning microscope coupled to an EDS Voyager X-ray spectrometer equipped with an SE secondary and BSE backscattered electron detector. Chemical composition analysis was performed by energy dispersive X-ray microanalysis (EDS) using a Thermo Noran detector.

Findings: Increased iron content in aluminium-silicon alloys is a major concern. It causes a significant reduction in the mechanical properties of the materials. This is due, among other things, to the increasing scarcity of primary materials (high cost and environmentally unjustifiable) versus the increasing share of recycled materials. Based on the study, AlSi10MnMg(Fe) alloys obtained under pressure with higher iron content (about 1% wt.), the optimal value of manganese addition is about 0.58% wt.

Practical implications: This research has shown that it is possible to use recycled Al-Si materials. The article presents one way to reduce the negative impact of iron addition to aluminium alloys as a result of reusing this type of material.

Originality/value: The article presents the effect of manganese addition on the selected aluminium alloy. It was determined that the addition of manganese in the amount of 0.58% wt. causes a significant reduction in the negative effect of iron phases. The article is intended not only for the academic community but also for specialists in the foundry industry.

Keywords: Die casting, AlSi10MnMg(Fe) alloy, Microstructure of Al-Si, Iron-containing intermetallic phases

Reference to this paper should be given in the following way:

J. Piątkowski, M. Hejne, R. Wieszała, Influence of manganese content on the microstructure and properties of AlSi10MnMg(Fe) alloy for die castings, Archives of Materials Science and Engineering 123/1 (2023) 5-12. DOI: https://doi.org/10.5604/01.3001.0053.9750

1. Introduction

Aluminium-silicon alloys of approximately eutectic composition with the addition of manganese and magnesium are most often used for the production of die castings for parts of internal combustion engines (e.g., head covers) or components of body and chassis support structures (so-called structural details). They are found under various trade names such as Silafont, Aural, and Castaman [1-5], in which the addition of magnesium is in the range of 0.2 to 0.4 wt.% and facilitates separation processes during heat treatment to the T6 state [6,7]. Adding manganese improves fatigue strength and plastic properties (especially for thin-walled structural parts) and reduces pressure mould welding.

These alloys also have an increased iron content (up to about 1.2 wt.%.), especially when the feedstock materials are of secondary origin [8,9]. Due to the EU's stricter policies on environmental issues, the degree of secondary materials will continue to increase in the coming years. Its increased proportion results in the crystallisation of brittle and morphologically unfavourable phases of the $Al_XFe_YSi_Z$ type, the worst of which, due to its propensity to form microcracks, is Al_5FeSi, often referred to as the -Fe phase [10-14]. Various additives are introduced to reduce the crystallisation of iron phases, the most common of which is manganese. It causes the transformation of β-Al_5FeSi phases into $Al_X(Fe, Mn)_YSi_Z$ type phases, which most often produce $Al_{15}(Fe, Mn)_3Si_2$ or $Al_{12}(Fe, Mn)_3Si_2$, greatly reducing the negative effects of iron. A multicomponent eutectic α(Al)+Al(Fe, Mn)Si containing an $Al_{19}Fe_4MnSi_2$ phase considered isomorphous to Al20Fe5Si2 can also crystallise. In these phases, manganese atoms occupy the positions of iron atoms [15]. The type of morphology of the $Al_{15}(Fe, Mn)_3Si_2$ phases, as reported in studies [16-18], varies and depends on the manganese content and the degree of overcooling of the alloy ΔT. At high ΔT, α-$Al_{15}(Fe, Mn)_3Si_2$ crystallises in the form of compact polygons and at slower cooling - in the form of the so-called "Chinese script." When introducing elements into Al-Si alloys to reduce the negative impact of iron phases, the so-called "sludge factor" and the Mn/Fe quotient are also important, the values of which are determined differently depending on the type of alloy, the technology of its preparation and the metallurgical purity of the batch components [19-22].

The literature presents many ways to reduce the negative impact of iron on the structure of aluminium-silicon materials, such as changes in the casting process, ageing or the introduction of appropriate additives to the material. It should be remembered that each time, the method is selected, depending on the final product itself as well as adapted to the technological process. The research results presented in the article relate directly to the manufacturing process of engine parts for mass production [23-25].

This study aimed to determine the effect of different manganese addition contents from 0.2 to 1.0 wt.%) on the microstructure, HB hardness and selected mechanical properties (UTS; YS; EL) of AlSi10MnMg alloy with increased iron content (about 1.0 wt.%). The proportion of iron in the tested alloy is so high because approx. 50% of the loads came from secondary materials [26,27].

To realise the adopted goal, the scope of the research included:

- metallographic studies,
- HB hardness tests and selected mechanical properties,
- results of slurry ratio and Mn/Fe quotient,
- summary and conclusions.

2. Testing methodology

The test specimens were cast on a Buhler Carat 3000 cold chamber testing machine. The pouring speed in the pouring

Table 1.
Averaged results of the chemical composition of the AlSi10MnMg(Fe) alloy

Alloy label	Si	Mn	Mg	Fe	Ti	Zn	Cr	Sr, ppm	other	Al
A	10.96	0.14	0.38	0.94	to 0.08	to 0.08	to 0.04	ca.140	to 0.05	rest
B	10.22	0.37	0.30	0.99	to 0.08	to 0.06	to 0.05	ca.130	to 0.05	rest
C	9.88	0.58	0.34	0.92	to 0.08	to 0.06	to 0.04	ca.130	to 0.05	rest
D	10.84	0.77	0.41	1.02	to 0.08	to 0.08	to 0.05	ca.140	to 0.05	rest
E	10.55	0.92	0.36	0.97	to 0.08	to 0.08	to 0.05	ca.140	to 0.05	rest

gap is 300 cm·s^{-1}, the piston path is 150 mm, the holding time in the mould is 60 s, the full cycle time is about 110 s, and the alloy temperature about 750°C. The alloy was modified with AlSr10 mortar (approx. 0.01 wt.% Sr). The tests were carried out in the post-T6 condition:

- supersaturation: 475±5°C/6h/ cold water cooling,
- artificial ageing: 170±5°C/3h/ageing in air.

Chemical composition tests were performed using a Foundry Master Compact 8 emission spectrometer. Static tensile testing at ambient temperature was carried out according to PN-EN ISO 6892-1 on an Instron 3382 using a 20:1 ratio and a constant tensile speed of 5 mm/min^{-1}. Tensile strength (UTS), conventional yield strength (YS), and per cent elongation after rupture of a proportional sample (EL) were determined from this test. Brinell hardness measurement was performed on a Zwick ZHF1, with a loading force of 250 N, with a 5 mm diameter ball for 35 s. Ten measurements were taken, discarding the two outliers, and the arithmetic mean was calculated from the remaining measurements.

Metallographic studies were conducted on a MeF-2 Reichert light microscope. X-ray microanalysis studies were carried out on a Hitachi S-3400 scanning microscope coupled to an EDS Voyager X-ray spectrometer equipped with a SE secondary and BSE backscattered electron detector. Chemical composition analysis was performed by energy dispersive X-ray microanalysis (EDS) using a Thermo Noran detector.

Qualitative phase analysis was performed using the ICDD file and the HSC program. Rietveld analysis used the DBWS 9807 program, and the Pearson VII function was used to describe the profile of the diffraction lines.

X-ray studies were performed using a Philips X`Pert diffractometer, using a λCuKα – 1,54178 Å lamp, (graphite monochromator for the wavelength from the copper anode) powered by 30 mA at 40 kV. The registration was performed using the "step-scan" method with a step of 0.04° and a counting time of 10 s, in the 2θ angle range of 20° to 140°. The gap on the incident beam was 1°, and on the deflected beam was 2°. Soller slits of 0.04 mm were used.

3. Results analysis

AlSi10MnMg(Fe) alloy was used for the study, and the individual castings, numbered 1 to 5, differed only in manganese content. For each material tested, 6 castings were made, and the results presented are averages. Table 1 shows the chemical composition of the alloys studied, and the microstructures are presented in Figure 1.

Observation of the microstructure of AlSi10MnMg(Fe) alloy (A), where the manganese content was 0.14%, shows that iron crystallises in the form of long (about 200 μm), lamellar phases β-Al_5FeSi (Fig. 1a). Their morphology makes them unfavourable phases, lowering the mechanical and especially plastic properties of Al-Si alloys. In modern mechanical vehicles, such structures are unacceptable, as they would lead to rapid damage to selected components through cracking. When the manganese content was increased to 0.37% (sample B) and 0.58% (sample C), the phase was found to crystallise in the form of dendritic or so-called "Chinese script" (Figs 1b, 1c), while when the proportion of manganese content was further increased to 0.77% (sample D) and 0.92% (sample E), in the form of compact lumps, as shown in Figures 1d and 1e.

Additional chemical tests and analysis of the XDR X-ray diffractogram revealed that after the introduction of manganese, the proportion of -Fe phases decreased in favour of α-$Al_{15}(Fe, Mn)_3Si_2$ phases, as presented in Figures 2, 3.

A static tensile test was performed in the following part, and a Brinell hardness test was carried out. Based on the tests, the values of mechanical properties (UTS; YS; EL) and hardness of the tested alloys with the chemical composition shown in Table 1 were obtained. Figure 4 shows the obtained test results.

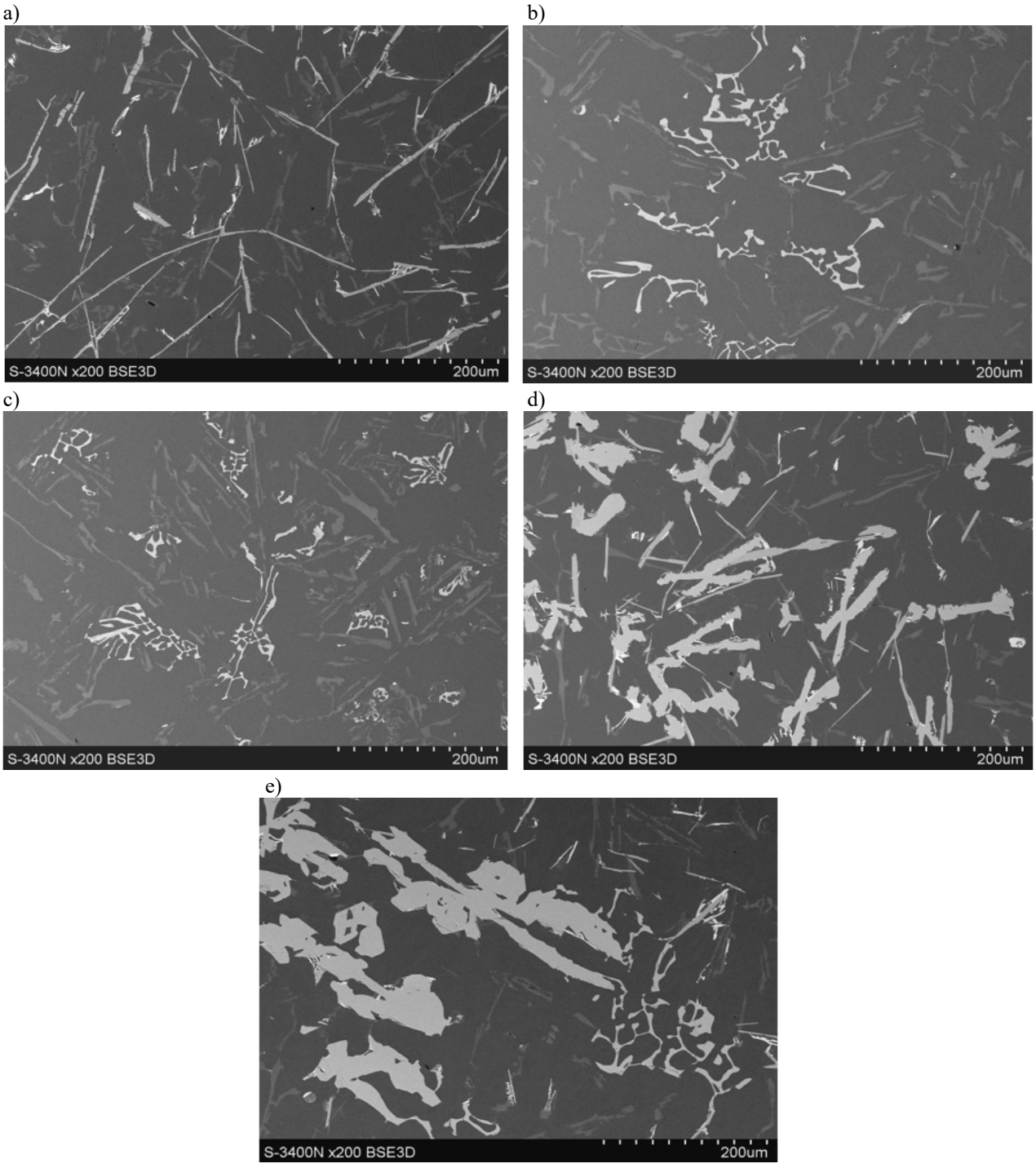

Fig. 1. Microstructure of the tested alloy at × 200 magnification, with different manganese content, according to Table 1: a) alloy (A), b) alloy (B), c) alloy (C), d) alloy (D), e) alloy (E)

According to the adopted purpose of the study, the values of the sludge factor (SF) and the Mn/Fe quotient were calculated for the studied alloys, as shown in Table 2. In the results of the SF factor, the proportion of chromium content was omitted since, according to the data in Table 1, it is below 0.05 wt.%.

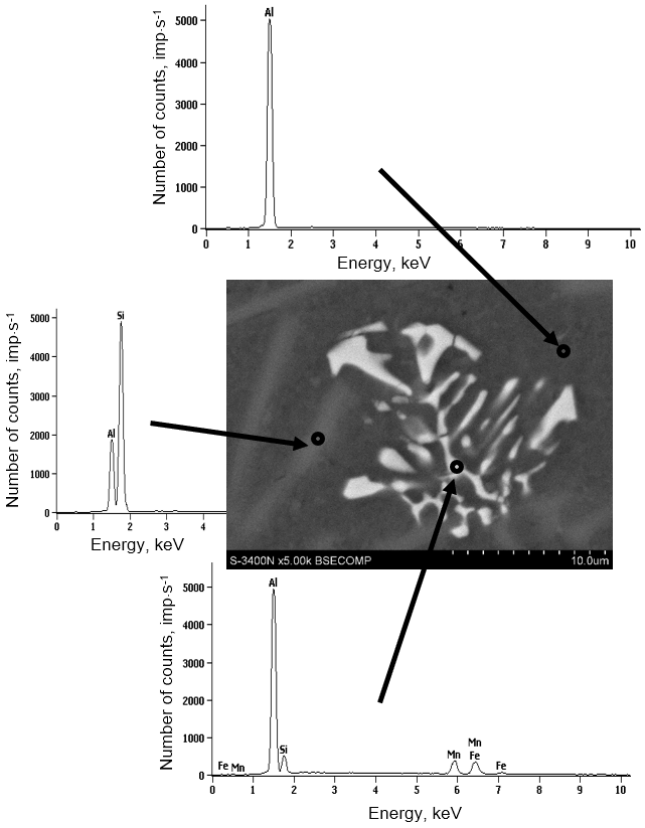

Fig. 2. Microstructure and results of microanalysis of chemical composition of (E) alloy

Polygons, combined with β-Fe phases, result in the formation of sludge, which is quite difficult to remove by conventional processes or metallurgical methods. To prevent this, the so-called "sludge factor" (SF - sludge factor) is calculated, the value of which depends on the proportion of iron, manganese, and chromium (if present in the alloy) and is determined by the relation [18]:

$$SF = wt.\%.\ Fe + 2\times wt.\%.\ Mn + 3\times wt.\%.\ Cr\ [\%]$$

Table 2.
Results of sludge factor (SF) and Mn/Fe quotient values of AlSi10MnMg(Fe) alloys with different manganese contents

Alloy label	wt. %.Fe	wt. %.Mn	SF	Mn/Fe
A	0.94	0.14	1.22	0.149
B	0.99	0.37	1.73	0.374
C	0.92	0.58	2.08	0.630
D	1.02	0.77	2.56	0.755
E	0.97	0.92	2.81	0.948

It is generally accepted that for Al-Si-Mn alloys SF should be about 1% (for castings obtained by gravity) and about 2% – for die castings. The study shows that such SF value was obtained for a content of 0.58wt. %.Mn (with about 0.92wt. %.Fe). Also important is the manganese/iron quotient, which is about 0.63 at the optimal SF content (Tab. 2). A higher value of SF and the Mn/Fe quotient cause the α-$Al_{15}(Fe, Mn)_3Si_2$ phase to start taking the form of thick lumps (Fig. 1), negatively affecting the mechanical properties of the tested alloys (Fig. 4).

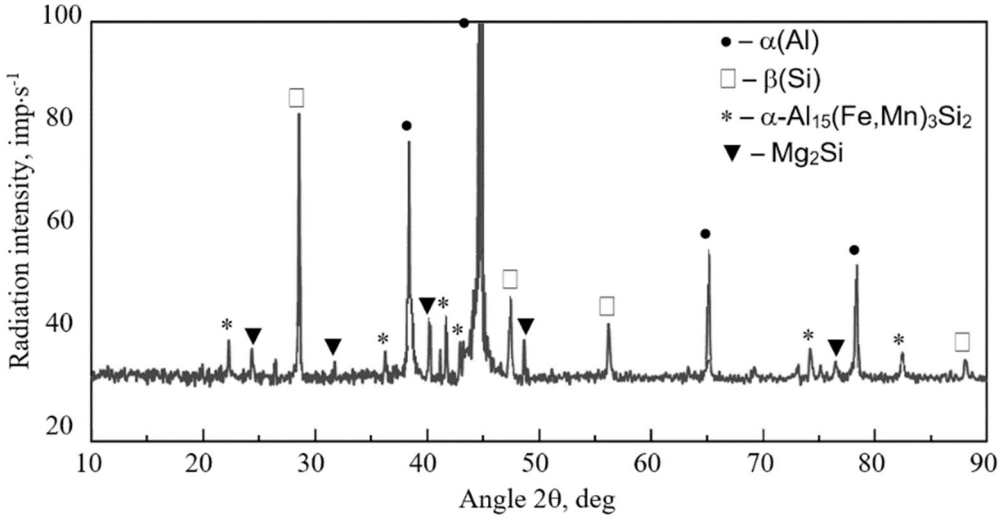

Fig. 3. XRD X-ray diffractogram of (E) alloy

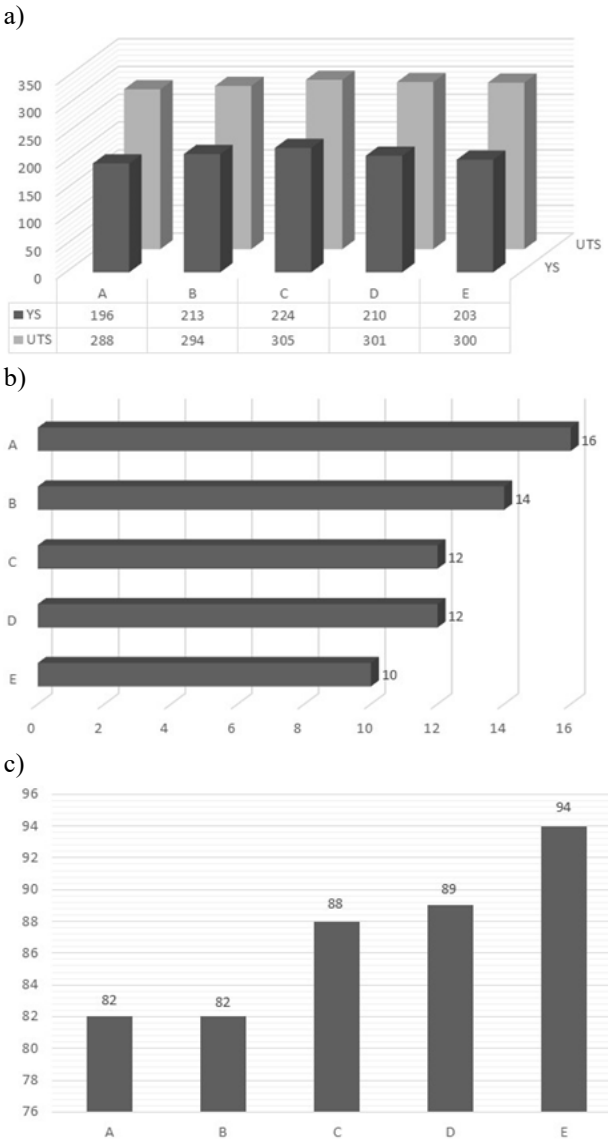

Fig. 4. Results: a) conventional yield strength (YS), tensile strength (UTS), b) relative elongation (EL), c) Brinell hardness

4. Conclusions

AlSi10MnMg(Fe) alloy with increased iron content (about 1% wt.) and increasing manganese content (from about 0.2 to 1.0% wt. in 0.2% increments) was selected for the study. General literature data show that manganese is the most common additive in silicas, the presence of which is intended to change the unfavourable morphology of β-Fe type phases into α-Fe, Mn type phases. The increased iron content, in turn, is a result of the increasing share of secondary raw materials at the expense of primary ones, which is in line with current trends of the growing importance of a closed-loop economy.

Based on the study, the following final conclusions were made:

1. For the studied AlSi10MnMg(Fe) alloys obtained under pressure with higher iron content (about 1% wt.), the optimal value of manganese addition is about 0.58% wt.
2. A higher proportion of manganese addition causes the α-$Al_{15}(Fe, Mn)_3Si_2$ phase with the morphology of the so-called "Chinese script" to start taking the form of thick lumps - which is unfavourable.
3. For the studied AlSi10MnMg(Fe) alloys, the optimal value of the SF ratio is about 2%, while the Mn/Fe quotient is about 0.6.
4. Exceeding these values results in the formation of unfavourable sludge, which reduces the strength and plastic properties.

It should be remembered that in the years to come, the problem of silumin iron contamination will continue to grow. This is due to the EU's environmental policy, which forces the use of recycled materials. On the one hand, there are plans to stop the production of piston internal combustion engines for automotive use in 2035, but this is a long way off, and secondly, on average, vehicles are currently in service for more than 15 years, which requires the preparation of an adequate number of spare parts. In addition, internal combustion engines are expected to stop being used in automotive vehicles and not in other industries such as air transportation. Piston engines used in small aircraft are similar in design to automotive engines, and therefore the demand from industry for research in this direction is constant and will continue to be needed for many years to come.

References

[1] Rhienfellden Alloys, Alloys for Pressure Die Casting. Available from: https://rheinfelden-alloys.eu/wp-content/uploads/2017/01/Handbook-Die-Casting-Aluminium-Alloys_RHEINFELDEN-ALLOYS_2016_EN.pdf
[2] J.R. Davis (ed), Alloying: Understanding the basics, ASM International, Materials Park, 2001.
[3] S.D. MacKenzie, G.E. Totten (eds), Analytical characterization of aluminum, steel, and superalloys, Taylor and Francis Group, Boca Raton, 2006.
[4] D. Bösch, S. Pogatscher, M. Hummel, W. Fragner, P.J. Uggowitzer, M. Göken, H.W. Höppel, Secondary Al-

Si-Mg high-pressure die casting alloys with enhanced ductility. Metallurgical and Materials Transactions A 46 (2015) 1035-1045.
DOI: https://doi.org/10.1007/s11661-014-2700-8

[5] Ł. Rudolf, M.T. Roszak, Tools of product quality planning in the production part approval process, Archives of Materials Science and Engineering 118/2 (2022) 67-74.
DOI: https://doi.org/10.5604/01.3001.0016.2591

[6] A.M. Samuel, F.H. Samuel, Effect of alloying elements and dendrite arm spacing on the microstructure and hardness of an Al-Si-Cu-Mg-Fe-Mn (380) aluminium die-casting alloy, Journal of Materials Science 30 (1995) 1698-1708.
DOI: https://doi.org/10.1007/BF00351598

[7] D. Zavadska, E. Tillova, I. Svesova, M. Chalupova, L. Kucharikova, J. Belan, The effect of iron content on microstructure and porosity of secondary AlSi7Mg0.3 alloy, Periodica Polytechnica Transportation Engineering 47/4 (2019) 283-289.
DOI: https://doi.org/10.3311/PPtr.12101

[8] L. Hurtalová, E. Tillová, M. Chalupová, E. Ďuriníková, Effect of chemical composition of secondary Al-Si cast alloy on intermetallic phases, Scientific Proceedings IX International Congress "Machines, Technologies, Materials", vol. 3, 2012, 23-26.

[9] L. Hurtalowă, E. Tillovă, M. Chalupowă, The structure analysis of secondary (recycled) AlSi9Cu3 cast alloy with and without heat treatment, Engineering Transaction 61/3 (2013) 197-218.

[10] P. Mikołajczyk, L. Ratke, Three dimensional morphology of β-Al_5FeSi intermetallics in AlSi alloys, Archives of Foundry Engineering 15/1 (2015) 47-50. DOI: https://doi.org/10.1515/afe-2015-0010

[11] F. Sanna, A. Fabrizi, S. Ferraro, G. Timelli, P. Ferro, F. Bonollo, Miltiscale characterisations of AlSi9Cu3(Fe) die casting alloys after Cu, Mg, Zr and Sr addition, Metalurgia Italiana 4 (2013) 13-24.

[12] X. Cao, J. Campbell, Morphology of β-Al_5FeSi phase in Al-Si cast alloys, Materials Transaction 47/5 (2006) 1303-1312.
DOI: https://doi.org/10.2320/matertrans.47.1303

[13] M. Mahta, M. Emamy, X. Cao, J. Campbell, Overview of β-Al_5FeSi phase in Al-Si cast alloys, in: L.V. Olivante (ed), Materials Science Research Trends, Nova Science Publishers, Hauppauge, 2008, 1-16.

[14] Ł. Chałada, M. Adamiak, A. Woźniak, Evaluation of anti-adhesive coatings on the surface of injection moulds made of Al alloys, Archives of Materials Science and Engineering 97/1-2 (2019) 5-11. DOI: https://doi.org/10.5604/01.3001.0013.2865

[15] G. Mrówka-Nowotnik, The role of phase components in shaping the microstructure and mechanical properties of aluminum alloys of group 6xxx, Publishing House of the Rzeszów University of Technology, Rzeszów, 2012 (in Polsh).

[16] R. Baldan, J. Malavazi, A. Cauto, Microstructure and mechanical behavior of Al9Si0.8Fe alloy with different Mn contents, Materials Science and Technology 33/10 (2017) 1192-1199.
DOI: https://doi.org/10.1080/02670836.2016.1271966

[17] S.G. Shabestari, The Effect of iron and manganese on the formation of intermetallic compounds in Al-Si alloys, Materials Science and Engineering A 383/2 (2004) 289-298.
DOI: https://doi.org/10.1016/j.msea.2004.06.022

[18] S.G. Shabestari, M. Mahmudi, M. Emamy, J. Campbell, Effect of Mn and Sr on intermetallics in Fe-rich eutectic Al-Si alloy, International Journal Cast Metals Research 15/1 (2002) 17-24. DOI: https://doi.org/10.1080/13640461.2002.11819459

[19] W.S. Miller, L. Zhuang, J. Bottema, A.J. Wittebrood, P. De Smet, A. Haszler, A. Vieregge, Recent development in aluminum alloys for the automotive industry, Materials Science and Engineering A 280/1 (2000) 37-49. DOI: https://doi.org/10.1016/S0921-5093(99)00653-X

[20] J.A. Taylor, Iron-containing intermetallic phases in Al-Si based casting alloys, Procedia Materials Science 1 (2012) 19-33.
DOI: https://doi.org/10.1016/j.mspro.2012.06.004

[21] S. Ferraro, A. Fabrizi, G. Timelli, Evolution of sludge particles in secondary die-cast aluminium alloys as function of Fe, Mn and Cr contents, Materials Chemistry and Physics 153 (2015) 168-179. DOI: https://doi.org/10.1016/j.matchemphys.2014.12.050

[22] S. Seifedine, I.L. Svensson, The influence of Fe and Mn content and cooling rate on the microstructure and mechanical properties of A380-die casting alloys, Metallurgical Science and Technology 27/1 (2009) 11-20.

[23] L. Zhang, J. Gao, L.N.W. Damoah, D.G. Robertson Removal of Iron From Aluminum: A Review, Mineral Processing and Extractive Metallurgy Review 33/2 (2012) 99-157.
DOI: https://doi.org/10.1080/08827508.2010.542211

[24] M. Tupaj, A.W. Orłowicz, M. Mróz, A. Trytek, Materials Properties of Iron-rich Intermetallic Phase in a Multicomponent Aluminium-Silicon Alloy, Archives of Foundry Engineering 15/1S (2015) 111-114.

[25] W. Khalifa, A.M. Samuel, F.H. Samuel, H.W. Doty, S. Valtierra, Metallographic observations of β-AlFeSi phase and its role in porosity formation in Al–7%Si

alloys, International Journal of Cast Metals Research 19/3 (2006) 156-166.
DOI: https://doi.org/10.1179/136404606225023372
[26] P. Puspitasari, R. Fauzan, T.L. Finta, M. Mustapha, D. Puspitasari, Morphology of aluminium with nickel addition on san casting process, Journal of Achievements in Materials and Manufacturing Engineering 87/1 (2018) 13-17.
DOI: https://doi.org/10.5604/01.3001.0012.0734
[27] T.B. Korkut, E. Armakan, O. Ozaydin, K. Ozdemir, A. Goren, Design and comparative strength analysis of wheel rims of a lightweight electric vehicle using Al6063 T6 and Al5083 aluminium alloys, Journal of Achievements in Materials and Manufacturing Engineering 99/2 (2020) 57-63.
DOI: https://doi.org/10.5604/01.3001.0014.1776